PERFORMANCE PREDICTION FOR THE WINDMILL WITH CAM-GUIDED BLADES

M.N. NAHAS*
M. AKYURT*

SUMMARY: Performance analyses are undertaken for a windmill that features cam-guided flaps. A single-flap windmill is treated as a slider-crank mechanism with variable eccentricity. The cylinder axis is also considered alterable. The resulting computer program is used in connection with the AL-YASEER software package to study the performance of the system under various wind as well as rotor speeds. The results obtained in this manner are compared with those of wind tunnel experiments on a physical model of the windmill.

Key Words: Al-Yaseer, Cam-Guided Flap, Slider-Crank Mechanism, Windmill.

A survey of windmills, conducted by the authors and associates (1), revealed that drag-type windmills offer certain advantages over others in numerous small-scale applications. Perhaps the best known of the former class is the Savonius rotor (Figure 1). It was noted that the returning blade in this rotor produces detrimental effects of performance. Recent studies (2,3) have focused on this issue in efforts to minimize the disturbance. The possibility of utilizing swinging blades (Figure 2) was investigated in this regard.

A fundamentally different concept was introduced (4) when then blades were allowed to execute general motion, instead of the purely rotative motion of existing windmills. This permitted the configuring of the returning of the blades so as to minimize the drag during this phase of the motion. Several different linkage designs were proposed for the execution of this task.

A special cam contour (5) was advanced next for the guidance of flaps (Figure 3), and with the purpose of eliminating of the negative effects during blade return. A model that incorporated the idea of cam guidance was physically constructed and then tested in a wind tunnel environment.

In what follows a windmill that features cam-guided flaps is studied, and predictions are formulated concerning the performance of such machines.

*From Mechanical Engineering Department, King Abdulaziz Unirvesity, P.B. Box 9027, Jeddah 21413, Saudi Arabia.

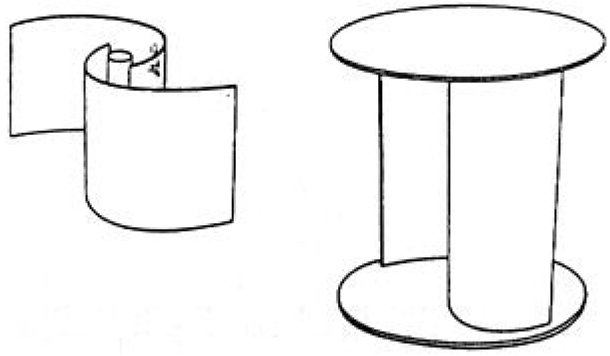

Figure 1: Savonius Rotor.

ANALYSIS

Referring to Figure 4, flap ABD is seen to drive the crank A. A under the action of wind force. F_u. Point B of the flap is in contact with a point on cam contour that has the instantaneous coordinates (x,y). Under ideal conditions, the flap would be perpendicular to the wind direction during the driving phase (Ω=0), and align itself so as to become parallel to it during the return phase. This would correspond to

$$x = r\cos\theta \quad (1)$$

$$y = r\sin\theta - 1/2 \quad (2)$$

during the drive phase, and

$$x = r\cos\theta + 1/2 \quad (3)$$

$$y = r\sin\theta \quad (4)$$

during the return phase. Eqns 1-4 define the cam contour

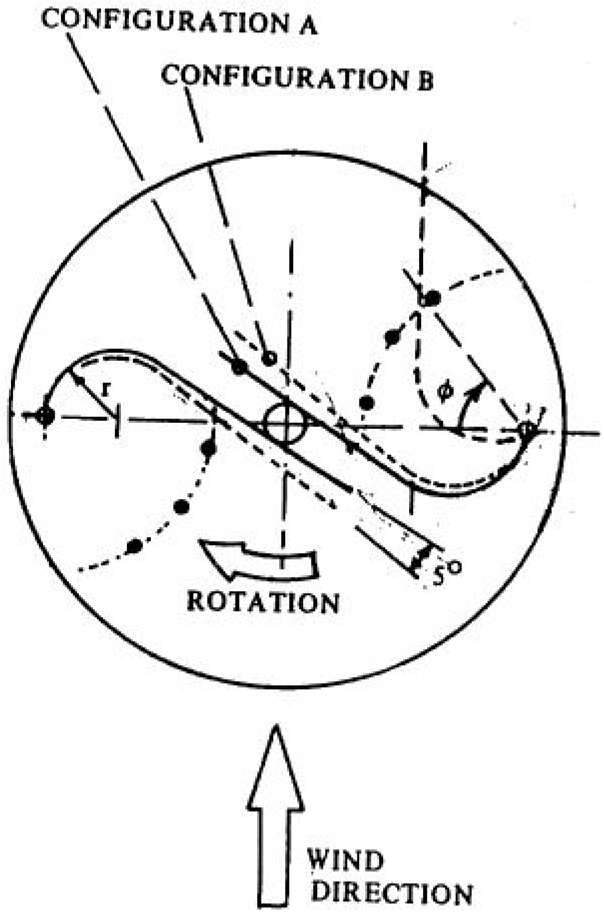

Figure 2: Savonius Rotor with Swinging Blades.

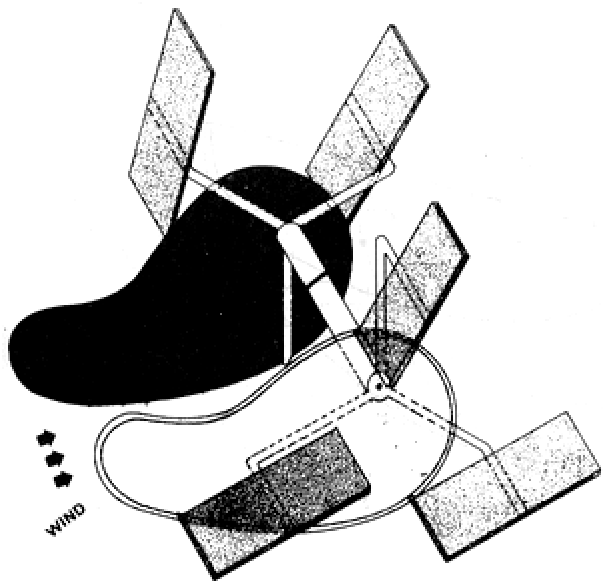

Figure 3: Windmill with Cam-Guided Blades.

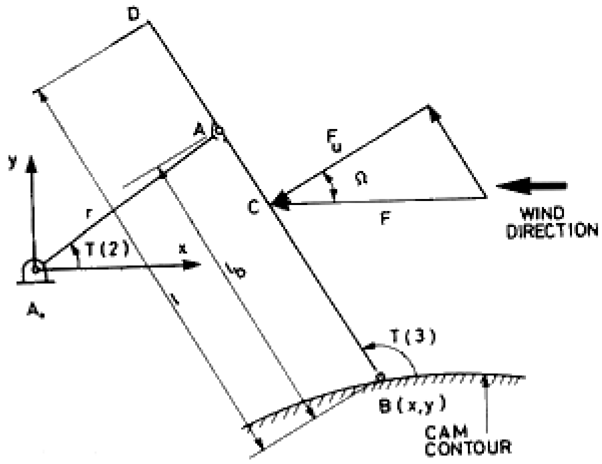

Figure 4: Flap Guiding Mechanism.

depicted in Figure 5. It is possible to conceive other contours, possessing various 1/r and 1_b/r values. Several alternative contours are presented in Figures 6, 7 and 8. The contour of Figure 8 represents the contour of the physical model that underwent wind tunnel testing (5). The same contour will form the basis of the analysis that follows.

Figure 9 shows the general slider-crank mechanism A_0AB of AL-YASEER (6), a dedicated soft ware package developed at King Abdulaziz University for the analysis of mechanisms and machinery. L (1) indicates the eccentricity, L (2) and L (3) the link lengths A_0A and AB, respectively and T (2), T (3) and T (4) are the inclinations of the crank, the connecting rod and the cylinder axis, respectively. All angles are positive when measured from the horizontal x-axis in the TAWAFWISE (counter-clockwise) direction. The first and second time derivatives of T(2) and T(3) are W(2), A (2) and W(3), A(3), in this order. R(2) and R(3) are used to locate the center of mass of the crank of mass M(2) and the connecting rod of mass M(3), respectively. H(2) and H(3) help locate the respective mass center with respect to L(2) and L(3). A(10) and A(11) depict the x and y components of the acceleration of M(2).

R(1), H(1) and R(4), H(4) help locate any other point of interest on the crank and on the connecting rod, respectively. Considering R(1), H(1) as an example, the x and y coordinates of the point located by R(1), H(1) are X(1), Y(1). Similarly V(1), V(2) and A(33), A(34) yield the x and y components of the velocities and accelerations of the same point.

P(1) designates a force acting on the piston. F(2) is an unknown force acting at a point R(1), H(1) of the crank, and F (9) acts on the connecting rod. Any given or known force on the crank is depicted in component form by F(0) and F(1). F(7) and F(8) are components of a known force

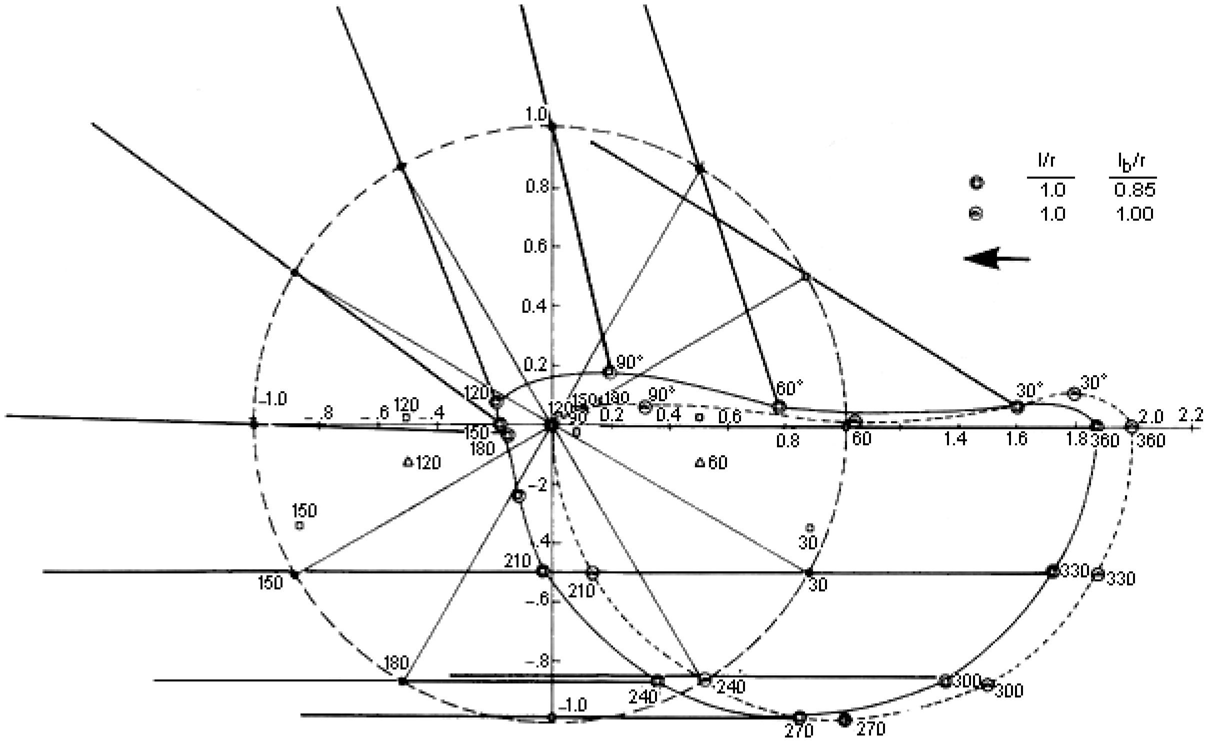

Figure 5: Cam Contour for 1_b /r= 1.0 and 0.85.

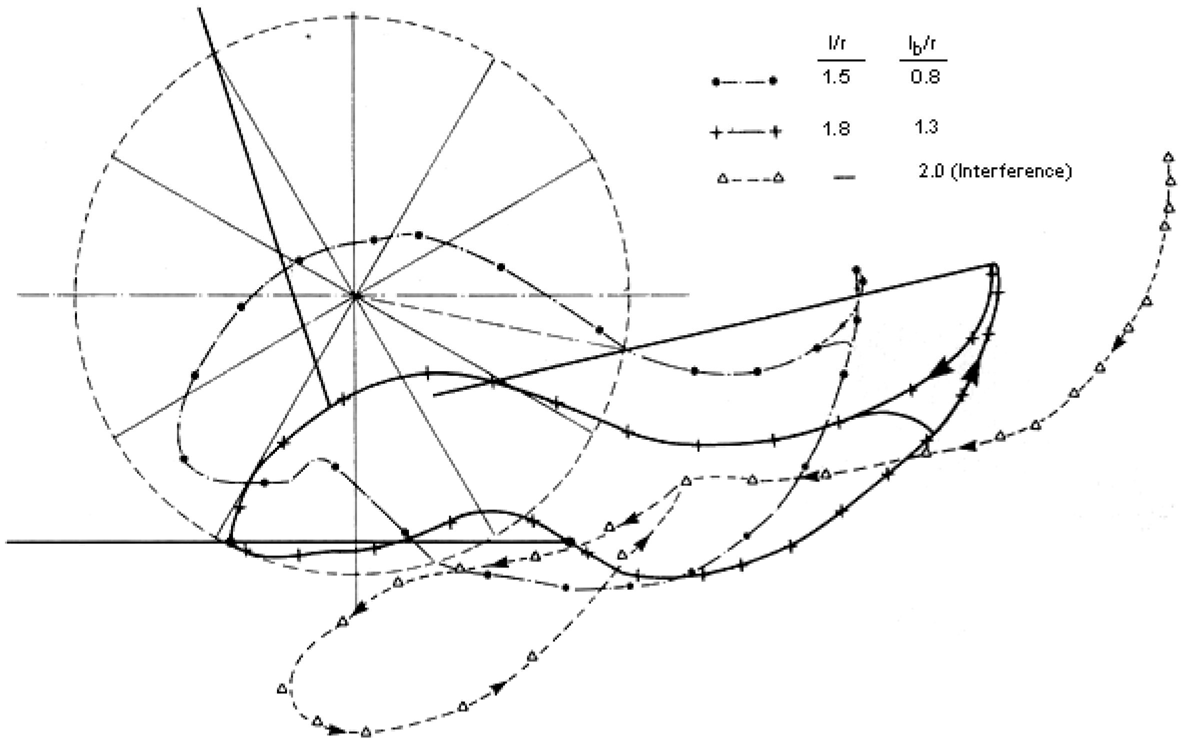

Figure 6: Cam Contour for 1_b /r= 0.8, 1.3 and 2.0.

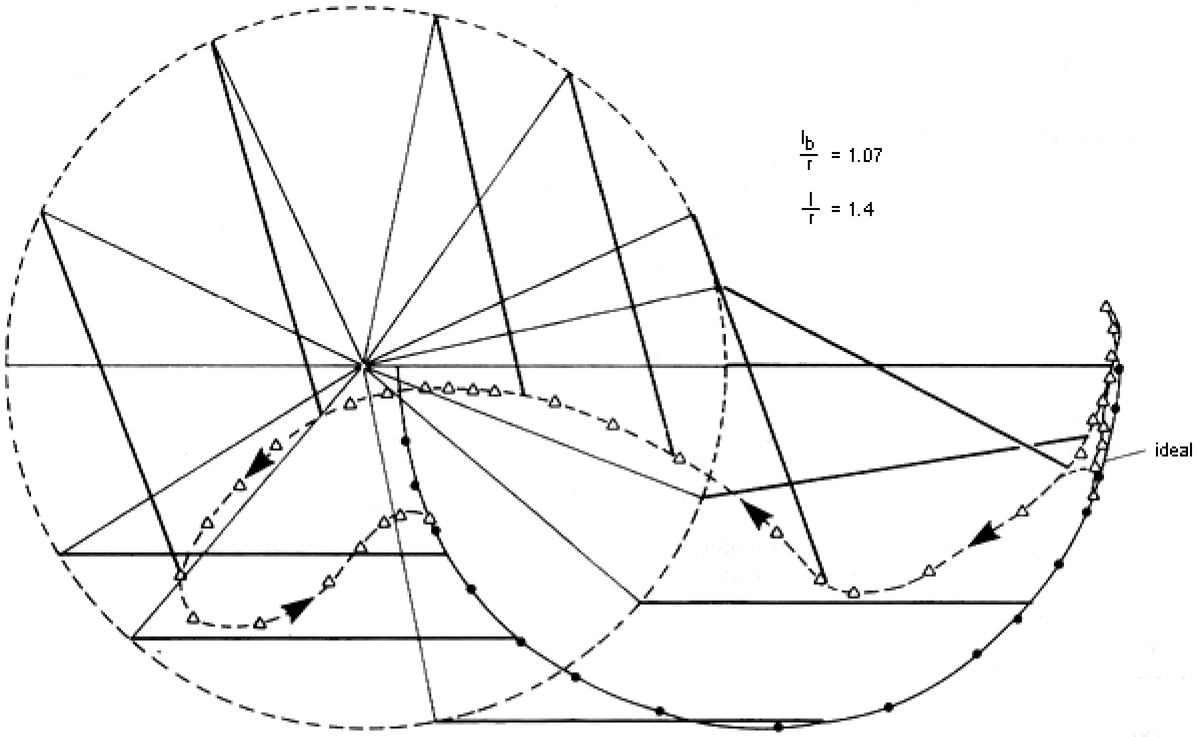

Figure 7: Cam Contour for 1_b /r= 1.07 and 1.4

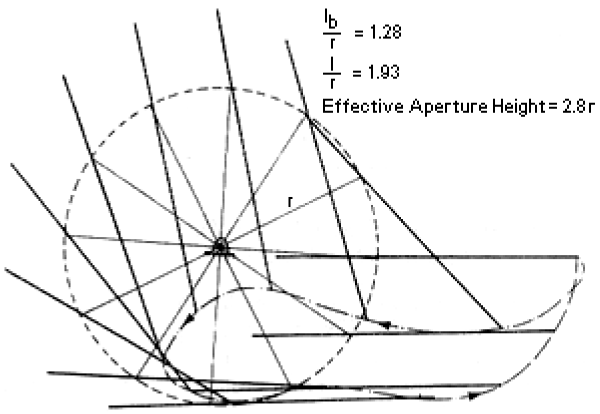

Figure 8: Cam Contour for 1_b /r= 1.28.

acting on the connecting rod. U(1) is a torque, positive as shown, acting on the crank. F(3) and F(4) are components of the resulting reactions at A_0. F (5), F(6) and F(10), F (11) are joint forces generated at the joints A and B, respectively. N(1) is the normal reaction at the cylinder.

Prog 1, where the information on the slidercrank mechanism of AL-YASEER is stored, as well as the rest of the subroutines of AL-YASEER are structured such that the computer does not necessarily run through the entire subroutine each time it is called. Thus if a static or quasi-static analysis is desired, an internal checking mechanism loops the computation outside the section on kinematics. In fact kinematics will be computed only if a nonzero value is specified to W (2), which is the angular speed of the crank. Force computations are initiated only if Z(1) is set equal to 2 by the user. In this case a value between one and four needs to be assigned to Q (1) to indicate to the computer what unknown external force or couple is to be solved for, i.e.; F(2), F(9), P(1) or U(1). All reactions and joint forces will then be automatically computed irrespective of the value assigned to Q (1). I(2) and I (3) denote the centroidal mass moment of inertia of the crank and the follower, respectively.

The wind force, F, acting on the flap may be characterized as

$$F= (1/2) \text{ as } (v^2_1 - v^2_2) \sin T (3) \quad (5)$$

where σ = air density

s = flap area

V_1 = wind speed

V_2 = velocity of point C on the flap (Figure 4).

The normal component, F_u, of the wind force may be conveniently expressed in terms of the external forces F(7) and F(8) and Figure 9:

F (7) = ABS (F) COS [T(3) +90]

F(8) = ABS (F) SIN [T (3) +90]

A brief program may now be written to invoke Prog 1 of AL-YASEER for the required computations. Tables 1 and

Figure 9: General Slider-Crank Mechanism.

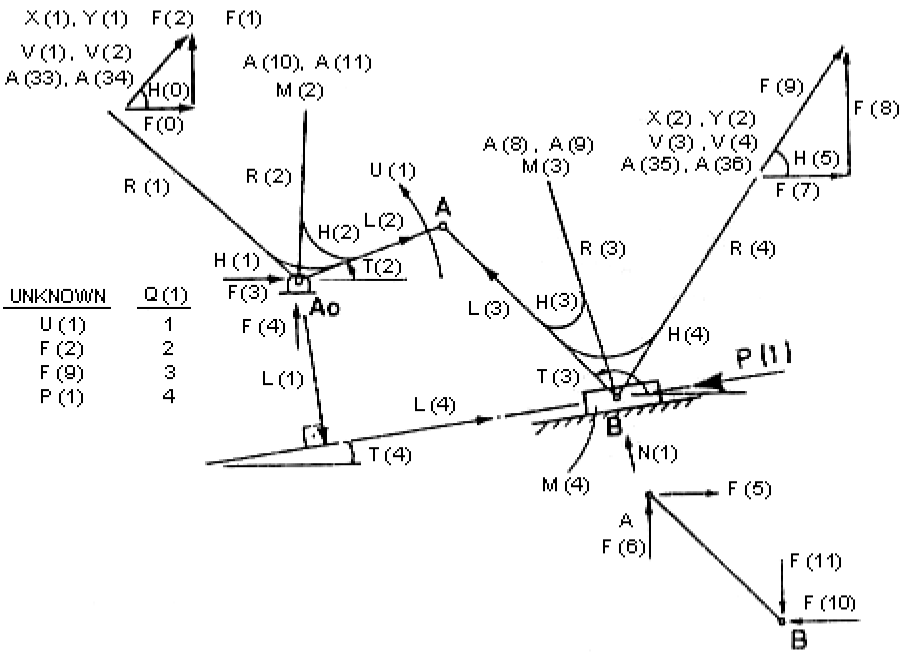

Table 1: Input Data for Computations.

Flap BD	width	0.20 m
	height	0.24 m
	area	0.048 m^2
	length of ABD	0.18 m
Crank A_oA	length	0.14 m
	mass (balanced)	1.00 kg
Connecting	length AD	0.06
Rod	length AB	0.18 m
	mass	0.60 kg
	moment of inertia	0.03 kg-m
Roller B	mass	0.07 kg

2 summarize the input data Figure 10 outlines the computation scheme in Prog 1, where a kinematic analysis is undertaken first, followed by dynamic analysis. The output may include position and kinematic information on the mechanism, as well as the crank torque, all joint forces, and bearing reactions.

RESULTS

Wind speed was varied from 3 m/s to 15 m/s, at steps of 3 m/s. For each wind speed, the speed of the rotor (angular velocity of the crank) was changed from 2 rad/s up to 10 rad/s at intervals of 2 rad/s. Typical results for an ideal single-flap machine with no mass and no friction are depicted in Figure 11. Figure 12 displays the variation of torque output with crank displacement for single and multi-flapped ideal wind machines.

It is clear that the upper limit of power available from a wind machine is the power developed by an ideal (massless, frictionless) machine. Figure 13 serves to illustrate the effect of having mass or no mass in a single-flap machine for a wind speed of 12 m/s. The system with masses is assigned the masses of the machine tested in the laboratory. The massless machine is the ideal wind-

Table 2: Input Data as Measured from Cam Contour (Figure 8).

Crank angle - 0	L (1) - m	T (4) - 0
0	0.000	0
30	0.050	15
60	0.015	0
90	0.025	0
120	0.032	220
150	0.052	260
180	0.150	-25
210	0.200	0
240	0.150	0
270	0.135	0
300	0.250	40
330	0.300	60
360	0.000	0

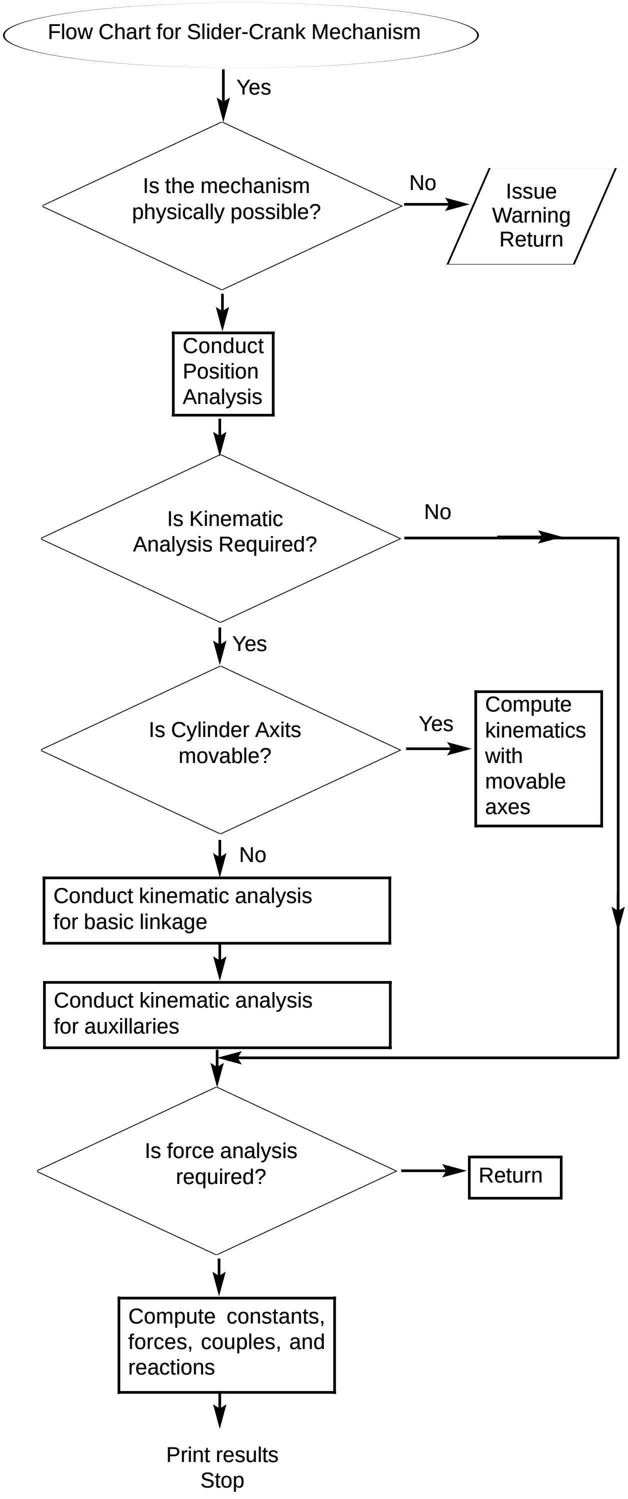

Figure 10: Flow Chart for AL-YASEER (PROG 1).

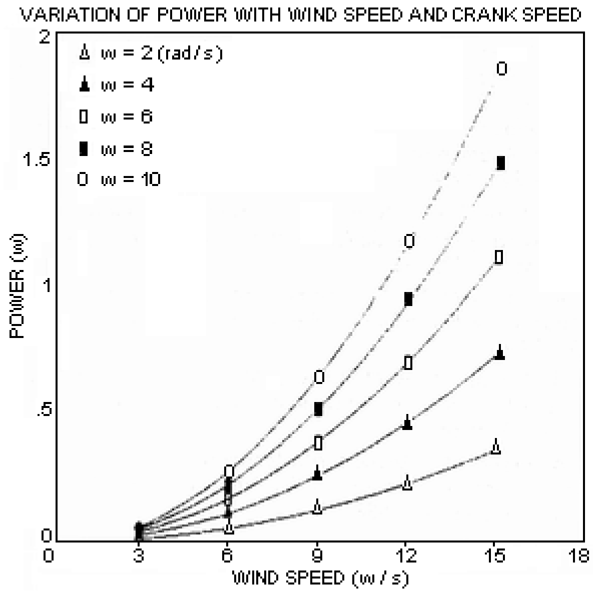

Figure 11: Variation of power with wind speed and crank speed.

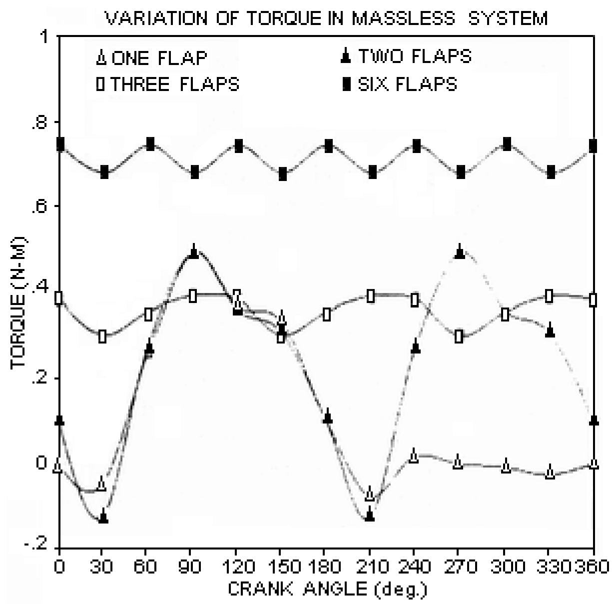

Figure 12: Variation of torque in mass-less system.

mill. The figure reveals that for any given power output, the machine with masses has a decidedly lower speed as compared to the ideal machine. Furthermore, it becomes manifest from Figure 13 that the machine with masses is limited by an upper speed, which for the current case is less than 6 rad/s. The ideal machine does not suffer from any such speed limitation.

DISCUSSION AND CONCLUSIONS

It follows from Figure 12 that, increasing the number of flaps on a machine, in general, has a dampening effect on fluctuations in power output during a given cycle. It may be shown, in fact, that for a machine with 12 flaps the fluctua-

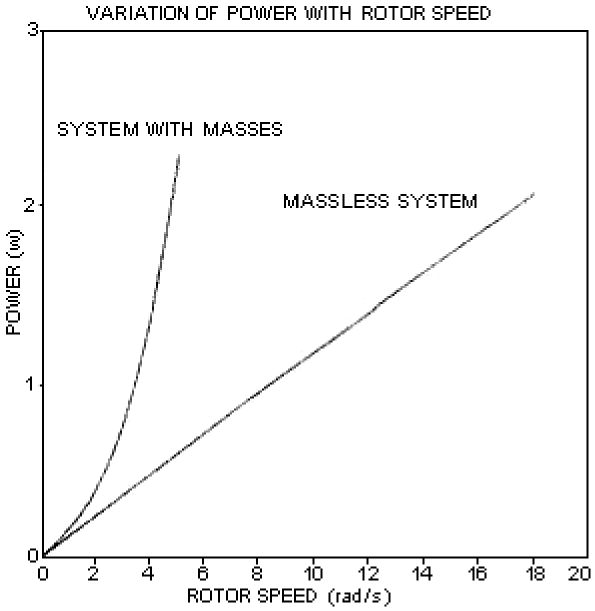

Figure 13: Variation of Power with Rotor Speed.

tions tend to die for all practical purposes. The arrangement of flaps must be in such a way as to not affect each other aerodynamically.

The predictions set forth in the current study fare well with the experimental results of Nahas and associates (5). For a windspeed of 12 m/s, these researchers measured a rotor speed of about rad/s, and a total power output of about 2.3 watts for six flaps. It may be safely stated that the power for a single flap machine would be about 2.3/4, or 0.6 W (5). Referring to Figure 13 with this value, it is observed that the predicted rotor speed is 2.8 rad/s. The predicted speed of on ideal machine would be about 5 rad/s under the same conditions.

The authors have found, in the same work (5), that the wind machine seems to have an upper speed limit of about 6 rad/s. That this is indeed the case may be readily verified from Figure 13, where it is observed that the limiting speed of the machine approaches asymptotically the value 6 rad/s, and this is for a wind speed of 12 m/s.

It is confirmed hence that it is sound to strive for reductions in mass and inertia of the windmill with cam guided flaps. It is further substantiated that modeling of this windmill as an offset slider crank mechanism with variable offset and tiltable cylinder axis is admissible. The predictions obtained by the use of this mathematical model, via the software package AL-YASEER, are acceptably close to the results of measurements made on a protatype physical model.

REFERENCES

1. Nahas MN, A Mohamed, M Akyurt, A El-Kalay: Wind Energyan Engineering Survey. Energy Sources 9(3):137-148, 1988.

2. Aldos TK: Savonius Rotor Using Swinging Blades as an Augmentation System. Wind Engineering 8 (4):214-220, 1984.

3. Aldos TK, YSH Najjar : Further Development of the Swinging-Blade Savonius Rotor. Wind Engineering 9 (3):165-170, 1965.

4. Nahas MN, A Mohamed, M Akyurt, A El-Kalay : Windmills with Articulated Blodes, Energy, 13 (3):275-280, 1988.

5. Nahas M, A Mohamed, M Akyurt, A El-Kalay : Windmills with Cam-Articulated blodes, Energy, 13 (6):499-508, 1988.

6. Akyurt M : Analysis of Mechanisms and Machinery, Department of Mechanical Engineering, King Abdulaziz University, Jeddah, 1988.

Correspondence:
M. N. Nahas
Mechanical Engineering Department,
King Abdulaziz University,
P.O. Box 9027, Jeddah 21413,
SAUDI ARABIA.